

Current distribution in HTSC tapes obtained by inverse problem calculation

M Carrera¹, X Granados², J Amorós³, R Maynou², T Puig², X Obradors²

¹ Dept. Medi Ambient i Ciències del Sòl, Universitat de Lleida, Jaume II, 69. 25001 Lleida, Spain

² Institut de Ciència de Materials de Barcelona, CSIC, Campus UAB, 08193, Bellaterra, Spain

³ Dept. Matemàtica Aplicada I, Universitat Politècnica de Catalunya, Diagonal 647, Barcelona, Spain

E-mail: mcarrera@macs.udl.cat, granados@icmab.es, jaume.amoros@upc.edu

Abstract. The development of SC devices based on HTSC tapes requires a deep knowledge of the current distribution in both pre-saturation and post-saturation regimes. Magnetic measurements have shown the possibilities to derive the current distribution by Inverse Problem Solution in finite sized bulks, based on a non destructive measurement of the magnetic field created by the own current flowing in the SC. In this work, the QR inversion strategy is extended to non finite systems by considering the effect of the boundaries. We present a method to derive the current distribution in a cross-section of a tape based on Hall magnetic mapping by using a specifically designed inverse problem solver. This method is applied to a series of Hall measurements corresponding to a full magnetization cycle of a commercial tape, produced by applying a set of the currents applied to the tape of several intensities. Details of the experiments and the calculation method are reported and the applicability as homogeneity test and losses studies is discussed.

1. Introduction

Quality control is one of the needs for the large scale production of reliable HTS tapes. There have been proposed several methods for non destructive in situ, or nearly in situ, testing of large length of tape. Determination of the critical current, J_c , by using reel to reel systems and measuring in short sections (typically 1-2 m) of the tape [1], Cryoscan system by using an induction coil as exploration probe[2], Magnetoscan system by measuring the magnetization footprint produced by a moving small magnet [3], or mapping the field trapped by tape by means of an external magnetic field by using a moving Hall probe or an array of them are examples of the effort due for development of such kind of systems. Although all the methods can detect possible defects and the subsequent reduction of the critical current, determination of the critical current map over the sample could give a better understanding of the actual effect of the possible defects in the tape, as has been proved in the analysis of bulks [4] by solving the inverse problem for a magnetic map provided by Hall probe scanning of the magnetized samples.

The aim of this work is just to design an adequate algorithm for obtaining the current distribution in a tape. The mapping of the magnetic field created by a transport current could constitute an interesting set of data that, converted into the original current map, gives a complete knowledge of the circulating current and its distribution showing so all the field penetration process associated. Simultaneous measurement of current and current density map could be achieved in this way. In the

present work we report on the inversion procedure and apply it to simulated and actual data measured over YBCO tapes by Hall mapping.

2. The inversion algorithm

The authors previously developed an inversion algorithm for the Biot-Savart problem in superconducting samples, both bulk and thin films, such that their critical current distribution is confined to the sample by its geometry. This inversion method is based on the discretization, linearization and QR-inversion of the resulting problem. Starting with a measurement of the vertical magnetic field B_z taken above the sample with a Hall probe, it derives the magnetization M as an intermediate step, and yields detailed 2-dimensional maps of the critical current J , averaged along the c -axis in the case of planarly chrystallized bulks [4,5,6,7].

In this work we introduce a new inversion algorithm for solving the inverse Biot-Savart problem in superconducting tapes, yielding a cross section of the current distribution on the tape deduced from Hall probe measurements of the magnetic field B_z above.

The challenge presented by solving the inverse Biot-Savart problem in tapes is that measuring the magnetic field above the entire circuit is unfeasible, thus one is forced to work with measurements of B_z above an open circuit, usually a small cross section of the tape.

Well-made superconducting tapes support a current that is rectilinear, in the direction of the axis of the tape, for most of the length of the tape, but may have localized irregularities affecting the direction of current circulation in some spots. In this note the authors show how to verify whether a given stretch of tape presents such localized irregularities or supports a rectilinear current by measuring the magnetic field B_z above the tape with a Hall probe.

As there are no sources or sinks of current in the tape, if the circulating current is *rectilinear* in the direction of the tape axis its density cannot vary in successive cross sections. I.e., if we set Ox to be the main axis of the tape and Oy its orthogonal axis a rectilinear current along the tape is of the form $J(x,y)=(J_x(y),0)$ (one single component, independent of x).

This note presents the algorithm that the authors have implemented to compute the current density J in a stretch of tape supporting a rectilinear current, using the Hall probe measurements of B_z above it. The tape may have either a thin superconducting layer or a thick one, chrystallized along the plane of the tape. In the later case, the average of the current density along the vertical axis is obtained.

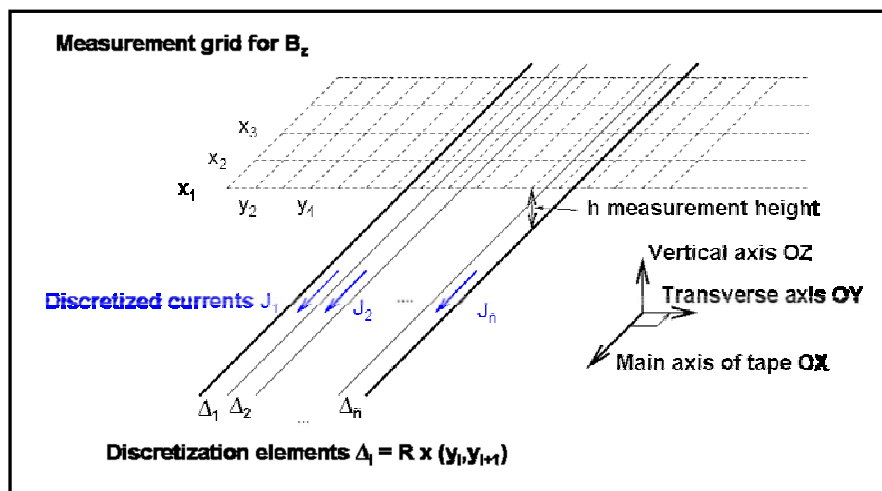


Figure 1. Graphic diagram of the tape discretization used in our inversion algorithm description.

The following is a concrete description of the algorithm (see figure 1):

- Measure with a Hall probe the vertical magnetic field B_z on a rectangular grid of *measurement points*, consisting of several parallel rows of points (x_j, y_k) ($j=1,2,\dots,m$; $k=1,2,\dots,n$), set orthogonally to the main axis of the tape.

- If the measured field B_z is constant along the main axis OX of the tape ($B_z(x,y) = B_z(x)$) for an interval (x_0, x_f) of length much greater than the height h at which the Hall probe is run above the sample then the circulating current J must be rectilinear.
- The stretch of tape on which the magnetic field B_z is constant along the main OX axis is then discretized by subdividing it in rectangular strips $\Delta_i = (x_0, x_f) \times (y_i, y_{i+1})$, with length the entire interval (x_0, x_f) along which J is rectilinear, and width comparable to the step size of the Hall probe measurements on each row transversal to the tape.
- Assume now that these thin strips $\Delta_1, \dots, \Delta_{\bar{n}}$ have infinite length, and a rectilinear current of constant density $J = (J_i, 0)$ on each of them ($i=1, 2, \dots, \bar{n}$). The vertical magnetic field generated by this current in a point $P = (x_b, y_b, h)$ is given by the Biot-Savart law as:

$$B_z(P) = \sum_{i=1}^{\bar{n}} \int_{\Delta_i} \frac{\mu_0}{4\pi} \frac{(\vec{J} \times \vec{r})}{|\vec{r}|^3} dx dy \quad (1)$$

Under our discretization assumption that $J = (J_i, 0)$ in every strip Δ_i , with J_i constant, and considering the strips to have infinite length, we may compute exactly every integral in (1), and the magnetic field induced in the point P is given by a linear combination of the current densities:

$$B_z(P) = \sum_{i=1}^{\bar{n}} \left[\frac{\mu_0}{4\pi} \ln \frac{(y_b - y_i)^2 + h^2}{(y_b - y_{i+1})^2 + h^2} \right] J_i \quad (2)$$

where y_i, y_{i+1} are the delimiting values for each strip Δ_i .

- Applying formula (2) to all points in the measurement grid where B_z is known yields a linear system of equations on the unknown densities $J_1, \dots, J_{\bar{n}}$.

In practice, it is advisable to take as a width for the discretization strips a multiple of the step for the Hall probe measurements, making the resulting system overdetermined. It is also advisable to make the height h of Hall probe measurements as small as possible. Following these recommendations results in a lower condition number for the resulting linear system, making the algorithm more robust with respect to measurement inaccuracies [5,6,7].

The above algorithm has been implemented by the authors, with a MATLAB program that computes and solves the resulting linear system. We start by presenting a simulated sample with geometry and dimensions which are typical of current superconducting tapes: our virtual tape has a width of 4.15 mm, and is subdivided in three substrips of equal width 1.38 mm. There is a rectilinear current circulation $J = (J_x(y), 0)$, with $J_x(y)$ given in each substrip by a sinusoidal curve as shown on figure *tallsJsimulacio*. The current circulating in the central substrip has total intensity 33.61A, and the lateral strips have a current of opposite sign and intensity 25% that of the central strip each. The global intensity of current in the tape is thus 16.81A.

The vertical magnetic field induced by this current has been computed to a great accuracy on a row of 201 points at a height $h=0.1$ mm, centered on, and transverse to the tape at its midpoint, with a total width of 10 mm, and a spatial resolution of 50 μm . Considering the tape to have infinite length, or to be 5 cm long with the measurement row in the center, results in values of the magnetic field B_z differing in less than 0.5%.

The following step has been to apply our inversion scheme to this simulated measurement of B_z , and compute a section of the current density J on the complete, 10 mm-wide, interval where B_z is known (so that no a priori assumption on the position or width of the tape is required), with a discretization step of 0.2 mm. The resulting linear system is 4:1 overdetermined, and has a condition number of 4.92, which means that a relative error of 0.5% in the value of B_z results in a relative error of 2.5% in the computed current density J .

Figure 2 shows the resulting current density J , compared to the original current density. The relative error with which J has been recovered is below 1.8%, and typically much smaller. The total intensity of the computed current is again 16.81A.

3. Application to YBCO tapes

The inverse Biot-Savart algorithm above described has been applied by the authors to study the current distribution in a commercial grade superconducting YBCO tape, made by Superpower. This tape

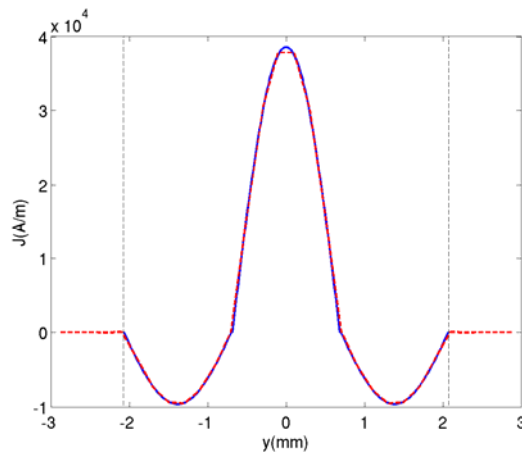


Figure 2. Current density in simulated sample. Computed current density J (red) and original imposed J (blue).

has a cross section of 4.15 mm. It contains a 1 μm -thick superconducting YBCO layer, with layers of Ag and Cu above with a combined thickness of about 24 μm , and isolating buffer layers made over Hastelloy substrate and a layer of Cu with a combined thickness of about 70 μm below the YBCO layer. A stretch of about 7 cm of this tape was inserted in a transport current circuit by fixing the beginning and end of the tape to blocks of Cu. The tape was then immersed in liquid N_2 at 77K, and the circuit was designed so that the current outside the tape was symmetrically distributed on both sides of the tape.

The tape was subjected to a ZFC process, and a transport current was applied then to the circuit, with total intensity varying in 3 cycles:

- (i) From zero to critical superconducting intensity: first, the intensity was increased from 0 to 122 A, at which intensity the transition to normal state according to the 1 $\mu\text{V}/\text{cm}$ criterion happened. The vertical magnetic field B_z was measured at intensities of 5, 10, 20, 30, 50, 70, 80, 90, 100, 110 A.
- (ii) From critical superconducting intensity to remanence: afterwards, the current intensity was decreased to 0 A, leaving the tape in a state of remanence. The magnetic field B_z was measured at applied intensities of 100, 80, 70, 50, 30, 20, 10, 0 A.
- (iii) From remanence to critical superconducting inverse intensity: finally, the direction of the applied current was inverted and increased. The magnetic field B_z was measured at intensities of -10, -20, -30, -40, -50, -60, -70, -80, -90, -100 A.

A Hall probe was rastered in several parallel rows, crossing the tape orthogonally to its main axis, at a height of 80 μm above the tape, i.e. 104 μm above the superconducting layer. The probe had an active area of 100 x 100 μm^2 , and the vertical magnetic field B_z above the tape was measured on each row with a steps of 50 μm . For each state of the tape, a rectangle was rastered above the central 4-4.5 mm stretch of tape, containing 5 or 10 rows of points 30 mm long across the tape. The difference between the 5 or 10 values of B_z at each cross section point of the tape was at most 0.45 G, and the graphs of B_z on the cross sections were parallel as figure 3, corresponding to the 10 rows measured in the initial cycle at an intensity of 10 A illustrates. The fluctuation of B_z between the different rows of the measurement lies within the resolution margin of the probe. Therefore we can regard the current going through the tape as rectilinear in the rastered stretch, and apply to it our algorithm to find the current distribution in a cross section.

Figure 4 shows a cross section of the magnetic field B_z at the end of cycle (ii), when the tape was brought to a state of remanence. The field has two symmetric peaks with values of $\pm 4.2 \times 10^{-3}$ T, and two smaller peaks at the edges of the tape.

Cycle (iii) of intensities provides interesting examples of the coexistence of different domains of current in the tape, and their evolution with the increase of the intensity of the applied inverse current.

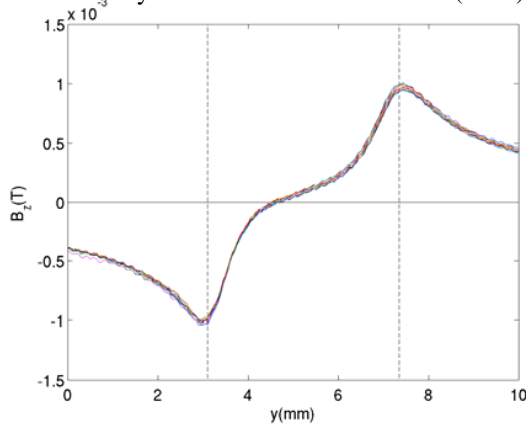


Figure 3. Magnetic field B_z measured at 10 parallel cross sections covering a central 4.5 mm stretch of the tape, with current intensity of 10 A in cycle (i).

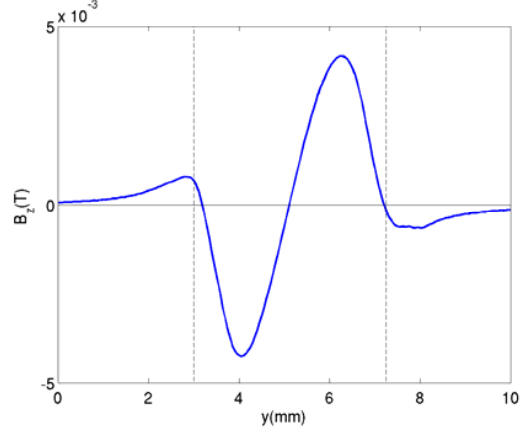


Figure 4. Cross section of the measured magnetic field B_z over the tape in state of remanence at the end of cycle (ii).

Our algorithm was applied to find the current distributions for each applied intensity in the 3 cycles of the tape. Figure 6 shows the current distribution in a cross section of the tape in remanence, and in the cycle (iii) when the inverse current is applied with increasing values of intensities of -10, -30, -50 A. For contrast, the current distribution on a cross section corresponding to the intensity of 50 A in cycle (i) is also included. For the sake of comparison, the figure shows a normalised current density, obtained dividing the current densities J for the intensities of 50, 0, -10, -30, -50 A by their respective maximum values of 1.1×10^4 , 7.8×10^3 , 8.3×10^3 , 1.1×10^4 , 1.4×10^4 A/m.

Figures 7 and 8 show the evolution of the current densities and domains in cycles (i) (increase of direct current from zero) and (iii) (increase of inverse current from remanence) respectively. In cycle (i) (specially at the initial intensities of 10, 20, 30 A) our algorithm detects an asymmetry in the cross section of J , which is greater in the edge of the tape at $y=3$ mm than in the edge at $y=7$ mm as figure 7 shows. The asymmetry fades in cycle (iii) (from remanence to -100A), as figure 8 shows. In cycle (iii), our computation of the current density J shows the coexistence of two current domains in the state of remanence, and how the inner domain vanishes when the applied inverse current reaches an intensity of -40A.

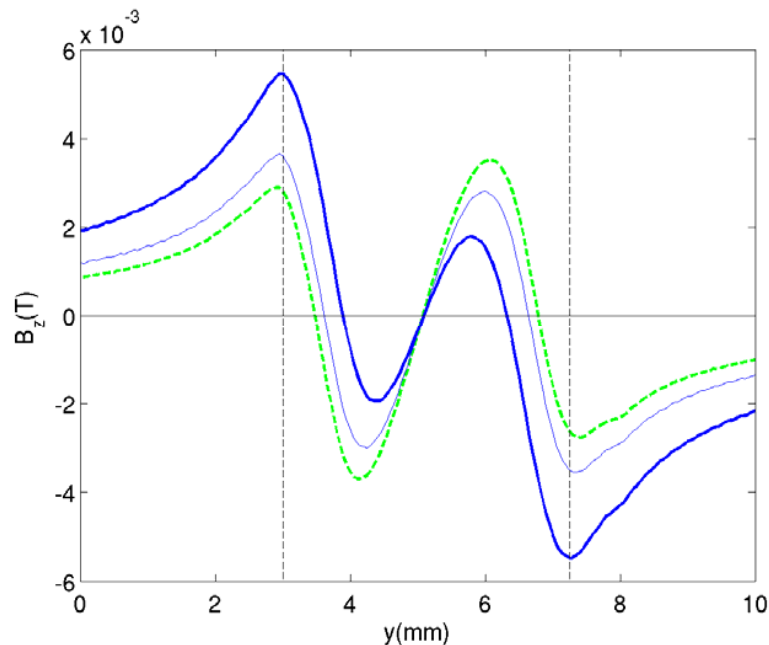


Figure 5. Evolution of the magnetic field on the tape when the inverse current is increased in cycle (iii): cross section of measured B_z at intensities -20A (green, dotted), -30A (blue, thin), -50A (blue, thick).

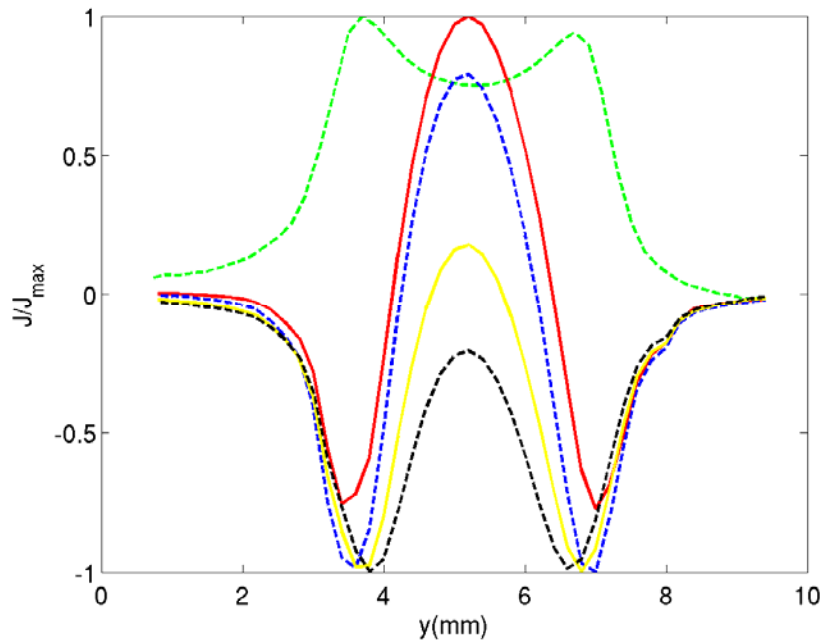


Figure 6. Normalized current densities in cross sections of the tape for the intensities of 50 A in cycle (i) (green, dotted); 0 A (red, continuous); -10A (blue, dotted), -30A (yellow, continuous), -50A (black, dotted) in cycle (iii).

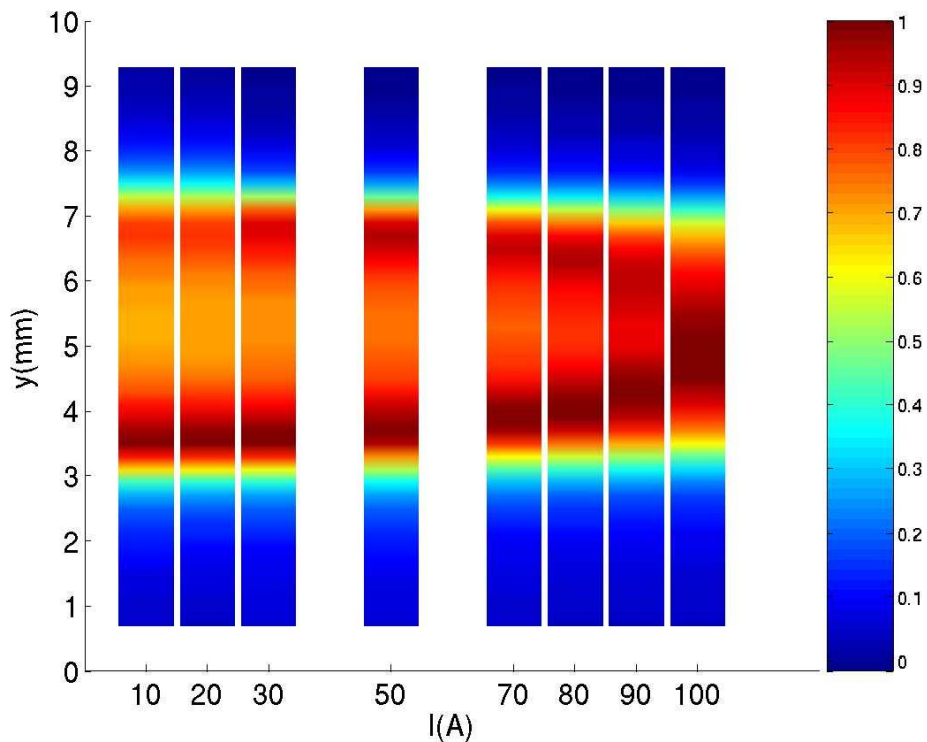


Figure 7. An increasing current is applied to the tape (cycle (i)). The normalized current density (J/J_{\max}) in a cross section on the tape reveals an asymmetry respect to the central axis.

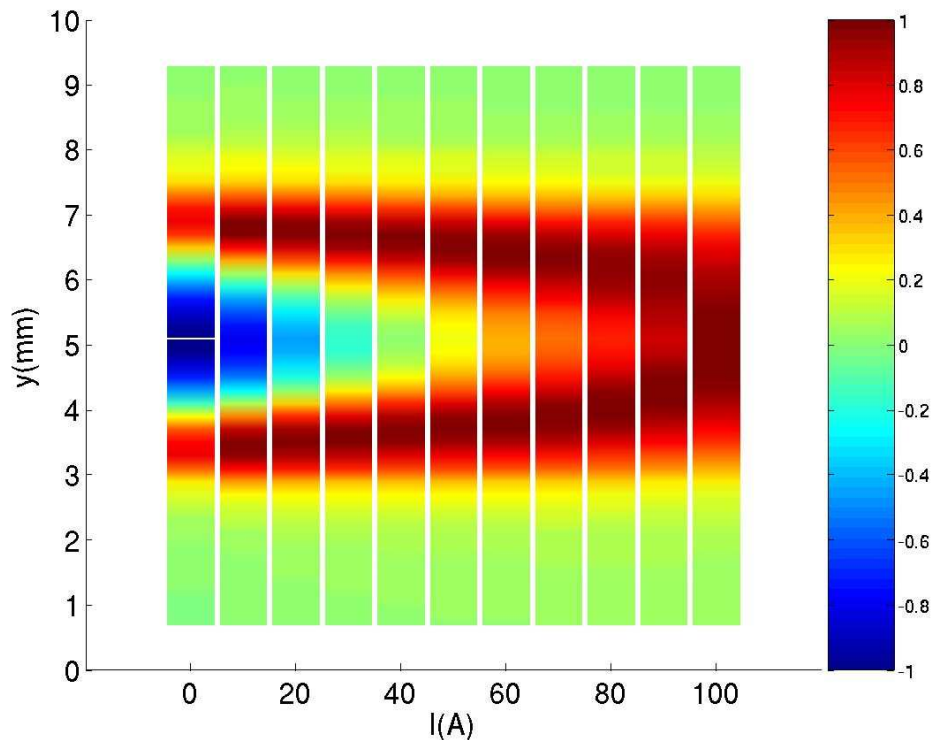


Figure 8. An increasing inverse current is applied to the tape in remanence (cycle (iii)). The normalized current density (J/J_{\max}) in a cross section on the tape shows how the inner domain of current in the remanence state of the tape vanishes when the applied inverse current reaches the intensity of -40A.

The authors have applied our inverse Biot-Savart computation scheme to the measurements of B_z in cross sections of the tape for 31 different applied intensities in the cycles (i),(ii),(iii) above described. The inversion of the 31 measurements, sharing the same geometry, was performed in a PC computer running MATLAB under the Linux OS, and took 3.2 ms of CPU time in total. The condition number of the resulting linear system for this inversion is 4.992. This means that, after J has been discretized, the relative error in the computed discretized J is at most 4.992 times the relative error in the measurements of B_z .

After the computation of cross sections of J , we may sum them to obtain the total intensity of current circulating through the tape according to our computation, and compare it with the actual intensity that has been measured in the circuit. Our algorithm has yielded in all cases a total intensity of current that is 85% of the real value.

Another test for our algorithm is that we make no a priori assumption about the tape position and width, so we can check the region where a significant current density is detected. This feature of the algorithm is necessary for the detection of regions in the sample where there is no current. In the case of the tapes reported here, as the figures 6, 7 and 8 show, our algorithm detects a significant current density J in a section of width about 5 mm, which compares to the actual width of 4.15 mm of the tape. This is a case of domain overspill error [5,6], related to the assumption that J varies discretely rather than continuously.

As a final validation, the authors applied the Biot-Savart law to compute the magnetic field B_z that the discretized current J yielded by our algorithm would induce at the points of the measurement grid of B_z . This recomputed B_z may then be compared with the originally measured B_z . Figure 9 shows the results of this comparison for two of the measures in the series, which display the typical behaviour of the complete series: the measured and recomputed magnetic fields B_z differ by 0.1 G or less above and around the tape.

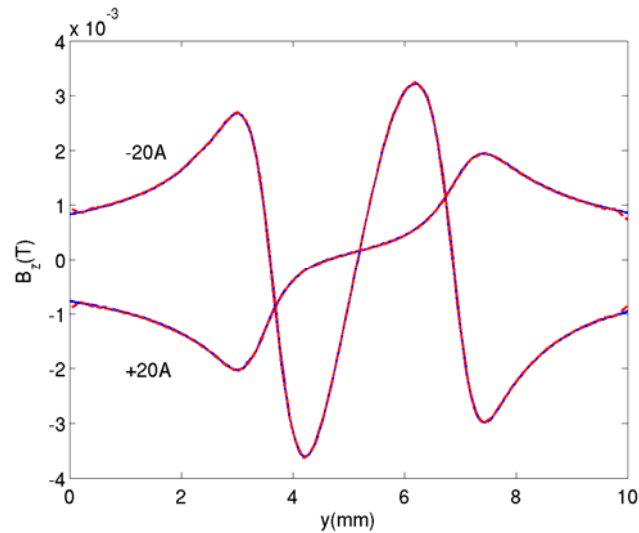


Figure 9. The measured (blue) and recomputed through our algorithm (red) magnetic fields for the measurements of B_z above the tape in cycle (i), intensity 20 A, and cycle (iii), intensity -20 A. The distance between the two curves is at most 0.1 G in each case.

4. Conclusions

The inverse Biot-Savart problem seeks to obtain a map of the current J circulating on a tape from measurements of the magnetic field $B_z(x,y)$ above it, serving as a quality control for the tape.

In a well-made tape, the current circulates rectilinearly (i.e. in the direction of the main axis of the tape) through most of the tape, and defects that affect the homogeneity of the tape and the direction of the current appear only in localized areas.

In this work we discuss first how to detect if a stretch of tape contains irregularities affecting the direction of the current: measure the vertical magnetic field $B_z(x,y)$ above the stretch of tape, in parallel rows that are transverse to the main axis of the tape. The current circulating through the stretch of tape is rectilinear in the direction of the tape main axis if and only if the measured magnetic field B_z has the same value in the parallel sections covering the stretch.

Next, we present an algorithm for the inversion in real time of the Biot-Savart problem in stretches of tape where the circulating current has the direction of the tape main axis, which takes advantage of this regularity to determine the density of the current in a cross section of the tape, making no other assumptions about position, size or regularity of the tape.

We show the effectiveness of this algorithm by applying it to both simulated samples and a commercial grade tape, which we study through cycles of applied current in a ZFC process going from zero to maximal applied current preserving superconductivity, to remanence, and finally to maximal applied inverse current preserving superconductivity. The evolution of the magnetic field B_z , measured with a Hall probe, and the current J on a stretch of tape are studied throughout the cycle, and as a final validation the magnetic field predicted by our computed current J is shown to coincide with the measured magnetic field. Our algorithm detects irregularities in the current density J of the real sample, such as an asymmetry or the evolution and vanishing of an inner domain of current when the applied current is increased gradually.

The case of a tape where the current is not rectilinear because there are localized defects will be studied by the authors as a continuation of this work. Applying the techniques of our prior work on 2-dimensional maps of the current density J in superconducting samples with current distribution confined to the sample by its geometry [5,6,7] and the procedure described in this work, we will complete the study of the current circulating through a tape with localized defects by determining 2-dimensional current maps around these defects that match up with the cross sections

of the current that we find in regular stretches of the tape in this note, all derived from a scan of the tape with a Hall probe.

Our techniques have been applied successfully to tapes with either a thin layer of superconducting material (as shown in this note) or a thick one. In the latter case, an average of the circulating current along the vertical axis is obtained.

Acknowledgments

Authors would like to acknowledge the support of NANOSELECT project funded by the Education Ministry of the Spanish Government.

References

- [1] Y. Xie, H. Lee, V. Selvamanickam. Patent US2006073977-A1; WO2006036537-A2; US7554317-B2
- [2] S. Furtner, R. Nemetschek, R. Semerad, G. Sigl, W. Prusseit, *Supercond. Sci. Technol.* 17, (2004) 281-284.
- [3] M. Zehetmayer, M. Eisterer and H.W. Weber, *Supercond. Sci. Technol.* 19 (2006) S429-S437.
- [4] M. Carrera, X. Granados, J. Amorós, R. Maynou, T. Puig and X. Obradors, *IOP J. Physics Conf. Series*, vol. 97 (2008).
- [5] M. Carrera, J. Amorós, A.E. Carrillo, X. Obradors, J. Fontcuberta, *Physica C* 385 (2003) 539
- [6] M. Carrera, J. Amorós, X. Obradors, J. Fontcuberta, *Supercond. Sci. Technol.* 16 (2003) 1187
- [7] M. Carrera, X. Granados, J. Amorós, R. Maynou, T. Puig and X. Obradors, *IEEE Trans. Appl. Supercond.* 19 (3) (2009) 3553-3556.